

Volatility Change During Droplet Evaporation of Pyruvic Acid

Sarah Suda Petters, Thomas G Hilditch, Sophie Tomaz,
Rachael E.H. Miles, Jonathan Philip Reid, and Barbara J. Turpin

ACS *Earth Space Chem.*, **Just Accepted Manuscript** • DOI: 10.1021/
acsearthspacechem.0c00044 • Publication Date (Web): 01 Apr 2020

Downloaded from pubs.acs.org on April 2, 2020

Just Accepted

“Just Accepted” manuscripts have been peer-reviewed and accepted for publication. They are posted online prior to technical editing, formatting for publication and author proofing. The American Chemical Society provides “Just Accepted” as a service to the research community to expedite the dissemination of scientific material as soon as possible after acceptance. “Just Accepted” manuscripts appear in full in PDF format accompanied by an HTML abstract. “Just Accepted” manuscripts have been fully peer reviewed, but should not be considered the official version of record. They are citable by the Digital Object Identifier (DOI®). “Just Accepted” is an optional service offered to authors. Therefore, the “Just Accepted” Web site may not include all articles that will be published in the journal. After a manuscript is technically edited and formatted, it will be removed from the “Just Accepted” Web site and published as an ASAP article. Note that technical editing may introduce minor changes to the manuscript text and/or graphics which could affect content, and all legal disclaimers and ethical guidelines that apply to the journal pertain. ACS cannot be held responsible for errors or consequences arising from the use of information contained in these “Just Accepted” manuscripts.

Manuscript for submission to *ACS Earth and Space Chemistry*

Volatility Change During Droplet Evaporation of Pyruvic Acid

3 *Sarah S. Petters,^{1*} Thomas G. Hilditch,² Sophie Tomaz,^{1,†} Rachael E. H. Miles,² Jonathan P. Reid,²*

4 *and Barbara J. Turpin¹*

5 ¹Department of Environmental Sciences and Engineering, Gillings School of Global Public
6 Health, University of North Carolina at Chapel Hill, Chapel Hill, North Carolina, USA

⁷ ²School of Chemistry, University of Bristol, Bristol BS8 1TS, UK

Keywords: secondary organic aerosol, multiphase chemistry, aerosol chemistry, aqSOA, carbonyl, vibrating orifice aerosol generator, aldol, cloud processing

10 **Manuscript for submission to ACS Earth and Space Chemistry. March 31, 2020.**

1
2
3
4
5
6
7
8
9
10
11
12
13
14
15
16
17
18
19
20
21
22
23
24
25
26
27
28
29
30
31
32
33
34
35
36
37
38
39
40
41
42
43
44
45
46
47
48
49
50
51
52
53
54
55
56
57
58
59
60

Manuscript for submission to *ACS Earth and Space Chemistry*

11 Abstract

12 Atmospheric water-soluble organic gases such as pyruvic acid are produced in large quantities by
13 photochemical oxidation of biogenic and anthropogenic emissions and undergo water-mediated
14 reactions in aerosols and hydrometeors. These reactions can contribute to aerosol mass by forming
15 less volatile compounds. While progress is being made in understanding the relevant aqueous
16 chemistry, little is known about the chemistry that takes place during droplet evaporation. Here we
17 examine the evaporation of aqueous pyruvic acid droplets using both the Vibrating Orifice Aerosol
18 Generator (VOAG) and an electrodynamic balance (EDB). In some cases pyruvic acid was first
19 oxidized by OH radicals. The evaporation behavior of oxidized mixtures was consistent with
20 expectations based on known volatilities of reaction products. However, independent VOAG and
21 EDB evaporation experiments conducted without oxidation also resulted in stable residual
22 particles; the estimated volume yield was 10–30% of the initial pyruvic acid. Yields varied with
23 temperature and pyruvic acid concentration across cloud, fog, and aerosol-relevant concentrations.
24 The formation of low volatility products, likely cyclic dimers, suggests that pyruvic acid accretion
25 reactions occurring during droplet evaporation could contribute to the gas-to-particle conversion
26 of carbonyls in the atmosphere.

27 Introduction

28 Aerosols affect global climate and impact air quality, human health, and visibility. A substantial
29 fraction of aerosol mass is organic, much of which is formed in-situ in the atmosphere. Despite its
30 ubiquity, predictions of secondary organic aerosol (SOA) formation rely on incomplete
31 mechanisms unlikely to capture aerosol production over a wide range of precursors and
32 conditions.^{1–3} Water-mediated reactions, occurring in humidified aerosols, fogs, and cloud
33 droplets, play an important role in converting water-soluble organic gases (WSOGs) to SOA

Manuscript for submission to *ACS Earth and Space Chemistry*

34 mass.^{4–6} However, the contribution of aqueous reactions to SOA mass remains uncertain due in
35 part to a limited understanding of precursors and limited laboratory results to parameterize
36 models.^{1,7–11} Quantifying the impacts of aqueous and multiphase chemistry on aerosol mass
37 remains challenging, and a more detailed understanding of product volatility is needed.

38 A significant fraction of low molecular weight acids, aldehydes and carbonyls dissolve into
39 cloud or fog droplets. In the absence of additional reactions, these WSOGs largely evaporate
40 during water evaporation; the trace amounts that remain in the aerosol phase are determined by
41 their partial pressure in the gas phase and activity in the aerosol matrix. However, multiphase
42 reactions can generate low-volatility products that are retained in the equilibrated aerosol. Several
43 important criteria determine whether aqueous processing can appreciably increase SOA mass: (1)
44 the precursor must be abundant, (2) it must have a high vapor pressure before aqueous reactions,
45 (3) it must have a high Henry's law coefficient and thus strongly partition into water, and (4) it
46 must react in the aqueous phase to form less volatile products.

To date many cloud- and fog-relevant studies have focused on the aqueous OH oxidation of a limited number of compounds meeting the above criteria, such as glyoxal,^{12–14} glycolaldehyde,^{15,16} methacrolein,¹⁷ acetic acid,¹⁸ methylglyoxal,^{19–21} methyl vinyl ketone,²² phenolic compounds,²³ and pyruvic acid,^{24,25} as well as studies focusing on oxidation by singlet molecular oxygen²³ and triplet excited states of oxygen,^{23,26} photosensitization,²⁷ and photoinitiation.²⁸ The volatility of the products, or the extent to which products remain in the particle phase after water evaporation, has been determined for some of these systems but not for pyruvic acid. Studies have also shown that non-radical reactions can yield low-volatility compounds in deliquescent aerosols,^{29–32} especially for glyoxal, methylglyoxal, and isoprene-derived epoxydiols.^{29–32} Because these systems rely on catalysis, formation of oligomers is sometimes reversible; irreversible formation of low-volatility

1
2
3
4
5
6
7
8
9
10
11
12
13
14
15
16
17
18
19
20
21
22
23
24
25
26
27
28
29
30
31
32
33
34
35
36
37
38
39
40
41
42
43
44
45
46
47
48
49
50
51
52
53
54
55
56
57
58
59
60
Manuscript for submission to *ACS Earth and Space Chemistry*

57 products are generally associated with radical^{4,33,34} or ring-opening³¹ reactions due to their higher
58 activation energy. Nevertheless, glyoxal and methylglyoxal form stable products in evaporating
59 solutions with or without inorganic catalysts^{30,32,35} due to the reactive dicarbonyl group.³⁵ These
60 and other accretion reactions occurring in the absence of photooxidation have been recognized as
61 an important contributor to organic aerosol.³⁶ Evaporation of droplets concentrates solutes, shifts
62 the solution pH, and can allow enhanced surface partitioning of surface-active compounds over
63 short timescales, enhancing reaction rates.^{32,37-41} The droplet air-liquid interface may also
64 accelerate reactions by confining molecules to specific orientations, enhancing their reactivity or
65 acidity,⁴²⁻⁴⁶ and molecular partitioning to the air-liquid interface and self-organization in the
66 surface layer can affect gas uptake and reaction rates.^{47,48}

67 Pyruvic acid is abundant in aerosols, fogs, and clouds, and is produced^{19,24,25,49,50}
68 photochemically in the atmosphere^{50,51} mainly through gas-phase oxidation of aromatic
69 hydrocarbons,⁵²⁻⁵⁴ biomass burning,⁵⁵ and aqueous OH oxidation of methylglyoxal.^{49,56} Pyruvic
70 acid has an intermediate volatility³⁴ and partitions between the gas and aerosol phases.^{51,53,57}
71 Studies of aqueous pyruvic acid processing have focused on photolysis^{26,56,58} and OH-radical
72 initiated photooxidation.^{24,25,59} Evidence for dark pyruvic acid accretion reactions from
73 environmental chamber studies shows that partitioning of pyruvic acid and other acids or carbonyls
74 to SOA exceeds expectations based on their high vapor pressures.^{52,60} Here we extend these studies
75 to include dark processing of pyruvic acid in evaporating cloud droplets.

76 **Method**

77 Pyruvic acid evaporation experiments followed two methods and spanned concentration ranges
78 from 10 μ M to 2 M. Vibrating Orifice Aerosol Generator (VOAG)⁶¹ Evaporation and Residual
79 Analysis (VERA) was performed for a series of solutions between 10 μ M and 20 mM, a

1
2
3
4
5
6
7
8
9
10
11
12
13
14
15
16
17
18
19
20
21
22
23
24
25
26
27
28
29
30
31
32
33
34
35
36
37
38
39
40
41
42
43
44
45
46
47
48
49
50
51
52
53
54
55
56
57
58
59
60
Manuscript for submission to *ACS Earth and Space Chemistry*

concentration range that reflects cloud concentrations and concentrations as cloud droplets evaporate. Additional pyruvic acid evaporation experiments were performed using an electrodynamic balance (EDB) at 2 M. The EDB concentration is relevant to deliquescent aerosols rather than clouds; the choice of concentrations for EDB experiments was dictated by instrumental constraints. For comparison, VERA experiments were also performed for other organic acids (10 μM –20 mM) and for aqueous pyruvic acid after OH-radical oxidation (300 μM pyruvic acid; fog-relevant concentration). An evaporation model was used to aid in the interpretation of data. VERA and EDB techniques, oxidation experiments, and modeling are described in the following paragraphs.

VOAG Evaporation and Residual Analysis (VERA)

Droplet evaporation experiments were performed for aqueous solutions of pyruvic acid (with and without OH oxidation) or other organic acids/carbonyls using VERA as described previously.¹⁶ VERA emulates cloud droplet evaporation by generating micron-scale droplets with very narrow size distributions (monodispersed and near cloud-relevant sizes),⁶² and evaporating them in a turbulent flow tube. Briefly, a VOAG (TSI 3450) was used to generate monodisperse droplets. Water evaporated rapidly (\sim 1 s) and size distributions of the organic residuals were detected in real time downstream by an aerosol spectrometer (GRIMM Aerosol Technik Ainring GmbH; model 1.109). Evaporation of the organic was used to quantify its vapor pressure. Modifications to the instrument liquid feed, orifice, and flow tube following Barr et al.^{63–65} are described in the Supporting Information (SI) alongside the measurement schematic (Figure S1); analysis is described below. A 20 μm orifice was used and produced 35 ± 0.053 μm droplets under typical conditions. For an involatile solute, solutions of 9.4 μM to 19 mM result in dry residual diameters (hereafter referred to as “nominal diameters”) of 0.30 to 3.9 μm . Equilibrium water

1
2
3
4
5
6
7
8
9
10
11
12
13
14
15
16
17
18
19
20
21
22
23
24
25
26
27
28
29
30
31
32
33
34
35
36
37
38
39
40
41
42
43
44
45
46
47
48
49
50
51
52
53
54
55
56
57
58
59
60
Manuscript for submission to *ACS Earth and Space Chemistry*

103 retention was estimated from molar volume^{66,67} and did not exceed 2–5% of nominal particle
104 volume. Calculation details and spectrometer calibration are described in the SI. Observed residual
105 diameters were taken as the peak of the measured size distribution. The evaporation process and
106 the influence of physicochemical properties are described in the Evaporation Modeling section
107 below.

108 **Evaporation in the Electrodynamic Balance (EDB)**

109 Pyruvic acid solutions were evaporated in an EDB as described previously.^{68–70} Aqueous
110 solutions of 2 M pyruvic acid in ultrapure water were prepared. The higher concentration was
111 necessary due to experimental constraints and is comparable to total organic carbon (TOC) in
112 deliquescent aerosols.⁷¹ Droplets were produced using a piezoelectric droplet-on-demand
113 generator and trapped in an electrodynamic potential well generated from two pairs of concentric
114 cylindrical electrodes. Trapped droplets evaporated in a 3 cm s⁻¹ N₂ gas flow at constant
115 temperature and relative humidity (RH). A green laser (532 nm) illuminated the droplet and the
116 scattered diffraction pattern was used to determine droplet size with a time resolution of 10 ms.
117 Experiments were performed at 10, 20, and 25°C. Additional tests included variable RH or a
118 different initial solvent. EDB experiments were conducted at the University of Bristol. Each
119 experiment was repeated 4–9 times.

120 **Oxidation and Product Quantification for Pyruvic Acid + OH(aq)**

121 Aqueous solutions of 300 μM (10.8 ppm-C) pyruvic acid were oxidized via OH radicals using
122 a water-jacketed 1 L photochemical batch reactor at 25°C as described previously and products
123 were quantified by ion chromatography.^{19,72} The pyruvic acid concentration is similar to the total
124 organic carbon found in fog water or polluted cloud water.^{73,74} Estimated steady-state [OH] was
125 ~5.5×10⁻¹² M during pyruvic acid oxidation.⁷⁵ Additional experimental details are provided in the

1
2
3
4
5
6
7
8
9
10
11
12
13
14
15
16
17
18
19
20
21
22
23
24
25
26
27
28
29
30
31
32
33
34
35
36
37
38
39
40
41
42
43
44
45
46
47
48
49
50
51
52
53
54
55
56
57
58
59
60
Manuscript for submission to *ACS Earth and Space Chemistry*

126 SI. Typical cloudwater [OH] is believed to be 10^{-13} M or lower.^{76,77} We used higher concentrations
127 to focus on OH initiated reactions and to access a wide range of equivalent atmospheric oxidation
128 timescales from minutes to days.⁷⁶

129 Aliquots of 10–12 mL were withdrawn at increasing time intervals and offline analysis was
130 performed within one day. Samples were analyzed for organic acids using ion chromatography
131 (IC; Dionex ICS-3000) and for TOC (Sievers M9). Evaporation experiments using VERA were
132 performed for a subset of aliquots directly and after serial dilution.

133 Evaporation Model

134 Evaporation of pyruvic acid solution droplets in VERA was estimated following Su et al.^{70,78}
135 and Bilde et al.^{79,80} A model description is included in the SI. Particle velocity relative to the gas
136 was assumed to be the terminal settling velocity⁸⁰ and the gas-phase concentration of organic was
137 assumed to be zero in the flow tube (we estimate it was < 2% saturated). Pyruvic acid diffusivity
138 in air was estimated to be 8.1×10^{-2} cm² s⁻¹ via the Hirschfelder equation.^{79,81,82} VERA was
139 emulated by modeling water evaporation from the droplet until reaching the organic nominal
140 residual diameter, then modeling organic evaporation until the time of observation by the
141 spectrometer. Modeled RH was 11% and measured RH was 10–13%. In addition to modeling
142 binary water-organic solutions, we modeled scenarios introducing a second solute with lower
143 vapor pressure (10^{-4} Pa) into the droplet. The modeled residual diameter is mainly controlled by
144 aqueous solution concentration, organic vapor pressure, evaporation time and RH.

145 Figure S2 shows the evaporation model for the VERA technique. After water evaporation the
146 “nominal diameter” of the residual organic particle is calculated from the initial solution
147 concentration assuming no evaporation of the organic (x-axis). However, because the organic

1
2
3
4
5
6
7
8
9
10
11
12
13
14
15
16
17
18
19
20
21
22
23
24
25
26
27
28
29
30
31
32
33
34
35
36
37
38
39
40
41
42
43
44
45
46
47
48
49
50
51
52
53
54
55
56
57
58
59
60
Manuscript for submission to *ACS Earth and Space Chemistry*

148 matter partially evaporates, the “observed diameter” (residual diameter observed by the
149 spectrometer), on the y-axis, is dependent on the organic vapor pressure.

150 Panel A shows the expected “observed diameter” for a pyruvic acid-like compound with
151 different assigned vapor pressures. The lines bend because evaporation is proportional to droplet
152 surface area. The line spacing shows the vapor pressure resolution for organics of similar size and
153 functionality. Vapor pressures (p^o) between 3 and 0.3 Pa are resolved under current operating
154 conditions. Panel B shows the result of adding an involatile second solute to the modeled droplets,
155 simulating the conversion of some of the pyruvic acid to a less volatile compound – one that does
156 not evaporate on the timescale of the measurement. The inset is a three-bin volatility basis set for
157 this setup, where bin 1 ($p^o \leq 0.3$ Pa) describes compounds that do not evaporate, bin 2 ($0.3 \leq p^o$
158 ≤ 3 Pa) describes compounds that partially evaporate, and bin 3 ($p^o \geq 3$ Pa) describes compounds
159 evaporating completely before detection.

160 Figure S2 shows the droplet size after 4.9 s of evaporation (the flow tube residence time), to
161 simulate what is measured by VERA. It does not show the time-resolved evaporation of multiple
162 solution components because VERA uses a fixed observation time and multiple experiments with
163 different concentrations to generate a plot of nominal vs observed diameter. The model is therefore
164 helpful in interpreting the data. The presence or absence of curvature in the observations is an
165 indication of the volume fraction of solute in each of the volatility bins shown in Panel B. If
166 observations include curvature, some component falls in bin 2 and its vapor pressure can be
167 determined with greater precision. In the absence of curvature, all components are in bins 1 and 3,
168 with the fraction in bin 1 shown by the angle of the line of observed diameters. For example, if the
169 angle is 0° (x-axis), all compounds are in bin 3 (evaporated), and if the angle is 45° (1:1 line), all
170 compounds are in bin 1 (did not evaporate). Evaporation data (nominal vs observed residual

Manuscript for submission to *ACS Earth and Space Chemistry*

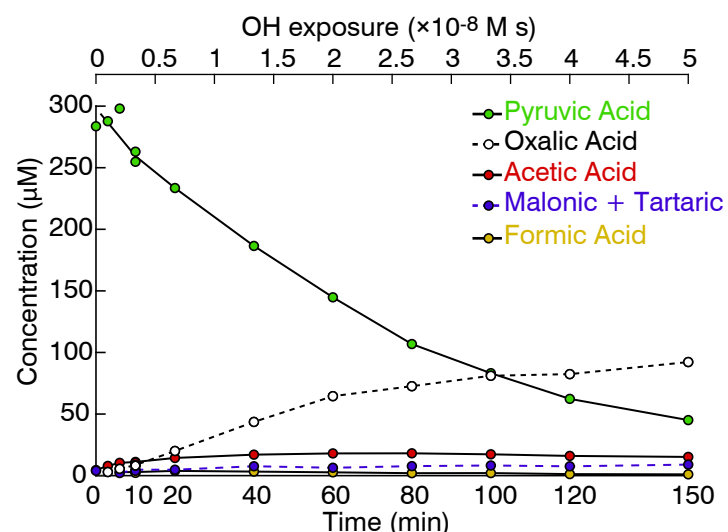
171 diameter) falling on a line between 0° and 45° in Figure S2 panel B are fitted and the slope of the
172 fit line is indicative of the fraction of organic that did not evaporate.

Results and Discussion

174 In the following paragraph we show that OH oxidation of pyruvic acid slowly produces acetic
175 and oxalic acids, consistent with known mechanisms, and that oxidation reduces the volatility of
176 the mixture. Then we present the dark evaporation of aqueous pyruvic acid using VERA and EDB
177 techniques. Despite expectations based on the vapor pressure of pyruvic acid, droplet evaporation
178 resulted in the formation of stable residual particles. A possible oligomerization mechanism and
179 atmospheric implications are discussed.

180 **Oxidation Experiments**

Figure 1 shows the evolving composition of 300 μM aqueous pyruvic acid undergoing OH radical-initiated oxidation over 150 min, as determined by ion chromatography. Oxidation converts pyruvic acid mainly to oxalic and acetic acid. This delayed formation of oxalic acid is consistent with the known multistep oxidation mechanisms.^{19,75,83} Evaporation of these solutions and their volatility is discussed below.



187 **Figure 1.** Oxidation products of pyruvic acid + OH(aq) as quantified by ion chromatography.

1
2
3
4
5
6
7
8
9
10
11
12
13
14
15
16
17
18
19
20
21
22
23
24
25
26
27
28
29
30
31
32
33
34
35
36
37
38
39
40
41
42
43
44
45
46
47
48
49
50
51
52
53
54
55
56
57
58
59
60
Manuscript for submission to *ACS Earth and Space Chemistry*

188 **VERA Evaporation Experiments**

189 Figure 2 shows the results of VERA experiments for oxidized pyruvic acid and for (dark)
190 standard solutions of pyruvic acid or other organics. As oxidation converts pyruvic acid to oxalic
191 acid, the net result is lower volatility, as seen by an increase in the slope of Figure 2A. By
192 comparing the slope of the observations with the modeled lines we estimate that the volume
193 fraction of organics in volatility bin 1 ($p^0 < 0.3$ Pa) was ~60% after 150 min of oxidation. The
194 remaining 40% was likely unreacted pyruvic acid and volatile products such as acetic and formic
195 acids. Panel B shows evaporated standard solutions. Most organics longer than 3 carbons did not
196 evaporate before observation and thus fall in bin 1 and are observed on the 1:1 line. Additional
197 experiments falling on the 1:1 line were omitted for clarity (glyoxal, glyoxylic acid, and malic
198 acids). Compounds evaporating completely fall in bin 3 ($p^0 > 3$) and are observed on the x-axis.
199 Pyruvic acid solutions evaporated partially (dark blue). As described in section 3, the lack of
200 curvature in the observation indicates that some of the solute was volatile (pyruvic acid falls in
201 volatility bin 3) and some of the solute did not evaporate (unknown compound falling in volatility
202 bin 1). Assuming volume additivity, ~10±5% of the pyruvic acid by volume was converted to a
203 lower volatility product. The volume conversion is likely lower when accounting for solvation
204 effects.

205

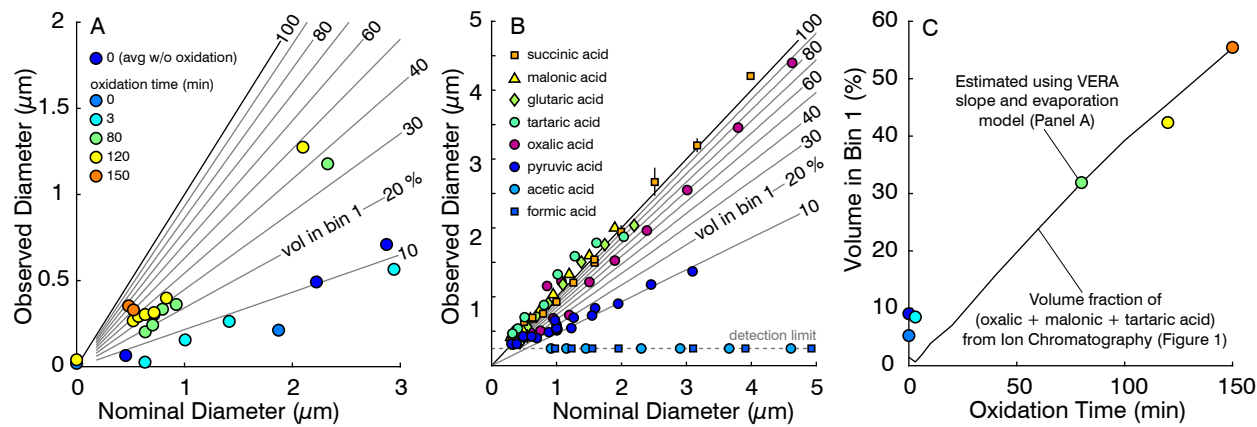
Manuscript for submission to *ACS Earth and Space Chemistry*

Figure 2. VERA evaporation of (A) oxidized pyruvic acid solutions (background subtracted) and (B) aqueous pyruvic acid and other compounds. Observed diameter is by spectrometer and nominal diameters are involatile-equivalent diameters from solution concentration. Grey lines show estimated fraction with lower volatility (volatility bin 1; $p^o < 0.3 \text{ Pa}$). (C) Percentage of solute in bin 1 ($p^o < 0.3$) estimated independently from VERA slope (circles; data from panel A) and from IC data (line; data from Figure 1).

Figure 2C shows that oxidation shifted products into the lower-volatility bin (bin 1). Colored circles indicate the fitted slope of VERA experiments in Panel A and the black line is an independent estimate of non-evaporating compounds for the same mixtures using ion chromatography, shown in Figure 1. The close agreement between these two estimates of evaporation corroborates the VERA model. The exception is near 0 minutes of oxidation, where evaporation of the pyruvic acid produced a 10% unknown residual (see blue circles, Figure 2C). Further experiments investigating this phenomenon were performed using the EDB and are detailed below.

EDB Evaporation Experiments

Figure 3 shows the evaporation of pyruvic acid solutions in the EDB. The sequential evaporation of water and pyruvic acid followed by the retention of an unknown low-volatility substance is clearly delineated by two sharp changes in evaporation rate (Panel A). Evaporation

Manuscript for submission to *ACS Earth and Space Chemistry*

rate slowed as remaining droplet constituents became less volatile. Abruptly raising the RH did not change the final residual diameter (Panel B). In the evaporation of pyruvic acid + isopropanol (Panel C) the sequential evaporation of solvent and pyruvic acid is also observed, again resulting in a less volatile residual. The volume conversion of pyruvic acid to low-volatility residual (assuming volume additivity and constant density equal to that of pyruvic acid) was ~15–30% across all EDB experiments.

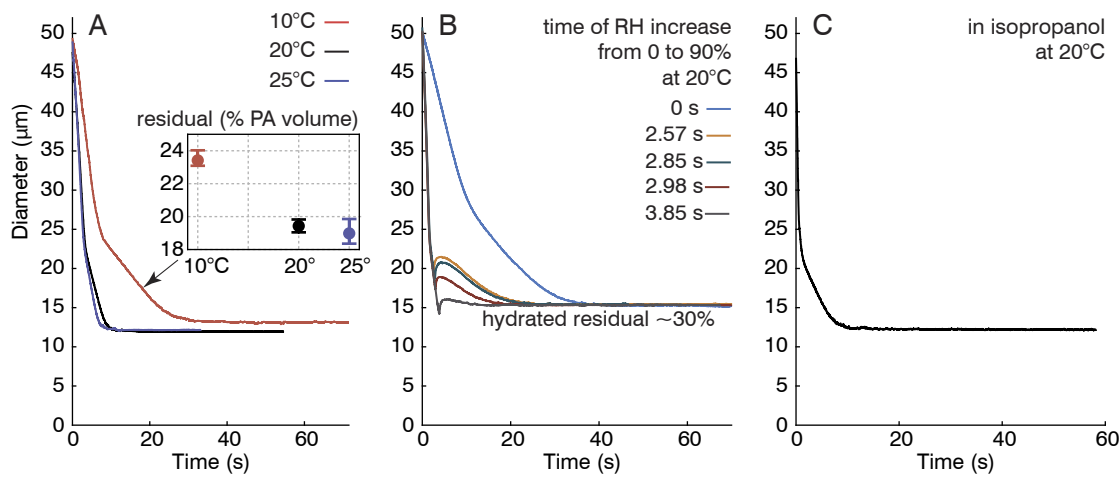


Figure 3. Evaporation of 0.1 mass fraction pyruvic acid solution droplets as observed by the EDB. (A) aqueous pyruvic acid evaporating in dry N₂ at three gas-phase temperatures. (inset) residual volumes at different temperatures. (B) aqueous pyruvic acid response to abruptly increasing RH during evaporation (at different times as indicated), (C) pyruvic acid in isopropanol evaporating at 20°C.

Varying experimental conditions affected the production of the low-volatility component.

Figure 3A shows that the residual volume of low-volatility product increases at colder temperatures, demonstrating that the sustained period of high pyruvic acid concentration in the evaporating droplet has a greater effect on the reaction rate than the reduction in molecular collisions expected at low temperatures. The volatility of the residual remained below the limit of quantification by EDB (<5×10⁻³ Pa) at all temperatures. Additional experiments operating on much

1
2
3
4
5
6
7
8
9
10
11
12
13
14
15
16
17
18
19
20
21
22
23
24
25
26
27
28
29
30
31
32
33
34
35
36
37
38
39
40
41
42
43
44
45
46
47
48
49
50
51
52
53
54
55
56
57
58
59
60
Manuscript for submission to *ACS Earth and Space Chemistry*

243 longer timescales would have been necessary to quantify the evaporation of the formed particles.
244 Although vapor pressure increases with increasing temperature, the effect of temperature-
245 dependent vapor pressure on the evaporation of a single compound would result in different
246 evaporation rates and not different yields. Higher initial droplet concentrations using the same
247 initial droplet size (VERA vs EDB) doubled the volumetric yield. When RH was increased from
248 0% to 90% at different times during droplet evaporation (Figure 3B), the observed residual
249 diameter was unchanged. Note that the residual here is larger due to equilibrium water uptake
250 (hygroscopicity estimate of $\kappa \sim 0.015$,⁸⁴ which is comparable to that of larger molecules found in
251 SOA⁸⁵). This indicates that changing the hygroscopically-bound water in the evaporating pyruvic
252 acid solution does not speed up the low-volatility product formation. In Panel C, evaporating the
253 pyruvic acid in pure isopropanol resulted in evaporation rates and residuals similar to those of
254 aqueous solutions, but a little higher (23±1% residual), perhaps reflecting slightly different
255 chemistry. Because carbonyls do not undergo hydration reactions to form gem-diols as readily in
256 isopropanol as they do in water, this suggests that the reaction producing the residual is not
257 accelerated by the formation of a gem-diol as observed for glyoxal.³⁵

39 40 41 42 43 44 45 46 47 48 49 50 51 52 53 54 55 56 57 58 59 60 **Proposed Mechanism for Self-Reaction of Pyruvic Acid**

259 Potential formation mechanisms and structures of a low-volatility residual are now discussed.
260 The residual volume is larger than the stated pyruvic acid impurity of 2% (all EDB experiments
261 used brand-new stock), and several independent sources of pyruvic acid standards produced
262 similar results. Some of this residual may form in the stock solution prior to use; however, the
263 changing volumetric yields with changing temperatures suggests that reactions occur during
264 evaporation experiments. Evaporation rates of the low volatility residual were below detection

1
2
3
4
5
6
7
8
9
10
11
12
13
14
15
16
17
18
19
20
21
22
23
24
25
26
27
28
29
30
31
32
33
34
35
36
37
38
39
40
41
42
43
44
45
46
47
48
49
50
51
52
53
54
55
56
57
58
59
60
Manuscript for submission to *ACS Earth and Space Chemistry*

265 limit, thus the influence of temperature on vapor pressure did not affect the observed yield. Gas-
266 phase impurities are ruled out with the EDB and are unlikely with VERA.

267 Pyruvic acid exists as several species in solution and these equilibria are shifted by the changing
268 pH during evaporation. The carboxylic acid group can deprotonate to form the pyruvate anion and
269 the keto group can hydrate to form a gem-diol or tautomerize to form an enol. At room temperature,
270 roughly 10% of pyruvate, or 60% of pyruvic acid, forms a diol.⁸⁶ Equilibrium between these forms
271 of pyruvic acid is complicated by the high surface-to-volume ratio and rapid removal of both water
272 and the volatile carboxylic acid form of pyruvic acid during evaporation of droplets.^{37,42,44}

273 The formation of C–O–C bonds by attack of an ROH group on the double bond of either the
274 carboxyl group or the keto group of pyruvic acid is plausible^{36,87,88} and oligoester products in SOA
275 have been observed in both laboratory and field studies.^{89,90} For example, the gem-diol of a
276 hydrated pyruvic acid molecule can attack the double bond of the carboxyl group of another
277 pyruvic acid molecule. In isopropanol, the isopropanol can attack the carboxyl double bond,
278 producing a similar ester (Figure 3C). Either isopropanol or the pyruvic gem-diol may attack the
279 hydrated keto group of another pyruvic acid molecule, forming a hemiacetal and potentially
280 repeating to form an acetal, as has been reported for glyoxal⁹¹ and 2-methylglyceric acid.^{89,90}
281 Formation of an acetal may be promoted by the removal of pyruvic acid and water from the droplet
282 during evaporation^{92,93} and enhanced acidity and reactivity in the surface phase.^{42,44,45}

283 Aldol addition and condensation reactions occur by the attack of the enol tautomer of pyruvic
284 acid on a protonated keto group of another molecule. Aldol addition has been proposed as a
285 thermodynamically favorable reaction in bulk aqueous systems,^{94–96} and these reactions are likely
286 accelerated at the droplet surface^{42,44,45} and by evaporation of water and pyruvic acid.^{92,93} Figure
287 S5 shows a proposed mechanism with a cyclic dimer as a potential end product of the aqueous

1
2
3
4
5
6
7
8
9
10
11
12
13
14
15
16
17
18
19
20
21
22
23
24
25
26
27
28
29
30
31
32
33
34
35
36
37
38
39
40
41
42
43
44
45
46
47
48
49
50
51
52
53
54
55
56
57
58
59
60
Manuscript for submission to *ACS Earth and Space Chemistry*

288 evaporation experiments in this work. Pyruvic acid tautomerizes readily in solution,⁹⁷ and aldol
289 addition can proceed without hydration of the keto group to a gem-diol. Self-reactions by aldol
290 addition have been reported for evaporating aqueous droplets of methylglyoxal and glyoxal³⁰ and
291 for pyruvic acid in both dark and photochemical reaction systems.^{56,98}

292 Atmospheric Implications

293 Pyruvic acid has diverse removal processes in the atmosphere, where it can partition between
294 aerosol, aqueous, and gas phases and can dissociate, hydrate, or tautomerize in solution. The
295 primary source of pyruvic acid outside of urban areas is the aqueous phase OH oxidation of
296 isoprene oxidation products such as methylglyoxal and lactic acid,^{19,57,99} and under dry conditions
297 it is found largely in gas phase (rather than the aerosol), where it is removed by direct photolysis
298 and dry deposition.^{51,53,100} In the presence of fogs and clouds pyruvic acid can be retained by (or
299 re-partition back into) the aqueous phase due to its high water solubility (Henry's law constant of
300 $3.1 \times 10^5 \text{ M atm}^{-1}$).¹⁰¹ The aqueous phase photochemistry is then competitive with the gas-phase
301 direct photolysis as a sink for pyruvic acid.¹⁰² In clouds and fogs, some pyruvic acid undergoes
302 OH oxidation to yield acetic acid, CO₂, and oxalic acid through a glyoxylic acid intermediate.¹⁹
303 Because of the multistep chemistry, conversion of pyruvic to oxalic acid takes hours and occurs
304 over multiple cloud cycles or in a persistent fog. Aqueous dehydrated pyruvic acid is light-
305 absorbing and can undergo direct photolysis or photosensitized reactions resulting in acetoin, lactic
306 and acetic acid, and oligomers through the excited triplet state of the carbonyl oxygen.^{26,28}
307 However, dark reactions in clouds and fogs can also occur. Dicarbonyls similar to pyruvic acid
308 such as glyoxal and methylglyoxal can oligomerize in evaporating droplets.^{29,30,32,35,88} This work
309 shows the potential for pyruvic acid to oligomerize during cloud and fog droplet evaporation.

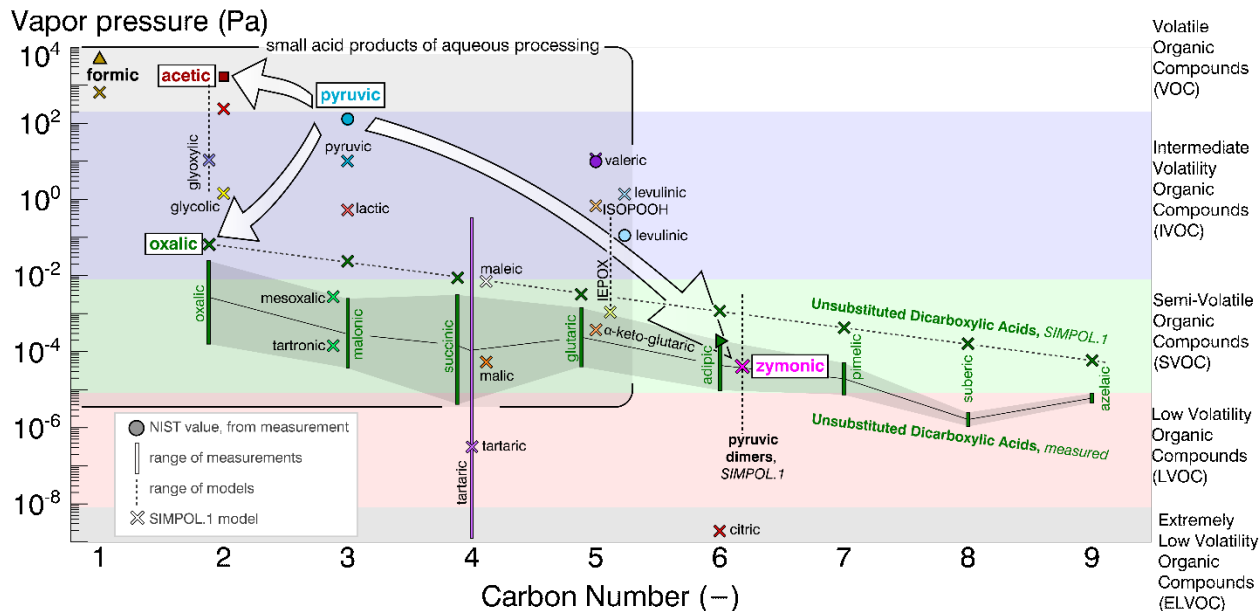
1
2
3
4
5
6
7
8
9
10
11
12
13
14
15
16
17
18
19
20
21
22
23
24
25
26
27
28
29
30
31
32
33
34
35
36
37
38
39
40
41
42
43
44
45
46
47
48
49
50
51
52
53
54
55
56
57
58
59
60
Manuscript for submission to *ACS Earth and Space Chemistry*

310 Figure 4 depicts the volatility evolution of aqueous solutions of pyruvic acid. The box in the
311 upper left-hand corner shows volatile and semivolatile carboxylic acids that are highly water
312 soluble, often result from aqueous oxidation, and partition readily into droplets. Processes reducing
313 the volatility of these compounds can increase the fraction of organic mass that remains in the
314 particle phase after water evaporation. Among these is pyruvic acid, with a vapor pressure of $\sim 10^2$
315 Pa at 20°C.^{103,104} Aqueous OH-radical initiated oxidation, dark acid-catalyzed accretion reactions
316 and, salt formation of pyruvic acid (not shown) have the potential to reduce the volatility of pyruvic
317 acid. Aqueous OH oxidation of pyruvic acid forms acetic acid, glyoxylic acid, and subsequently
318 oxalic acid, whose vapor pressure is in the semivolatile range ($p^0 = 10^{-2}$ to 10^{-4} Pa).^{105,106} The
319 preference of oxalic acid for the particle phase in the atmosphere is likely due to the formation of
320 low volatility oxalate salts or complexes.^{4,12,107} This work suggests that evaporating pyruvic acid
321 solution droplets at aerosol, fog, cloud-relevant concentrations and atmospheric temperatures (10–
322 25°C), in the absence of an inorganic catalyst, leads to formation of acetals and/or cyclic dimers
323 with estimated vapor pressures of 4×10^{-5} Pa¹⁰⁸ and 10–30% volumetric yields. This mechanism
324 could compete with photochemical sinks for pyruvic acid during cloud cycling.

325 Although the vapor pressure of dimers of pyruvic acid is significantly lower than that of pyruvic
326 acid, they are still considered semivolatile or low-volatility compounds. Dimerization enhances
327 the partitioning of monomers to the condensed phase.³⁶ The formed dimers, especially those with
328 unsaturated double bonds, can participate in additional condensed-phase reactions. For example,
329 the pyruvic acid dimers shown in Figure S5 have been shown to partition to the air-water
330 interface,¹⁰⁹ where they may have enhanced reactivity for subsequent reactions.³⁸ The formation
331 of surface active unsaturated dimers from carbonyls such as pyruvic acid during cloud or fog

Manuscript for submission to *ACS Earth and Space Chemistry*

332 evaporation is one way in which carbon can be transformed in the atmosphere and influence
 333 atmospheric chemistry.



334
 335 **Figure 4.** Vapor pressures of pyruvic acid reaction products compared to past organic
 336 measurements (20°C),¹¹⁰ SIMPOL.1¹⁰⁸ -estimated vapor pressures, and volatility ranges defined
 337 by Donahue et al.³⁴ Pyruvic dimers include several multifunctional cyclic acids (Figure S5).

1
2
3
4
5
6
7
8
9
10
11
12
13
14
15
16
17
18
19
20
21
22
23
24
25
26
27
28
29
30
31
32
33
34
35
36
37
38
39
40
41
42
43
44
45
46
47
48
49
50
51
52
53
54
55
56
57
58
59
60
Manuscript for submission to *ACS Earth and Space Chemistry*

338 **Supporting Information.** Instrument modifications and schematic; oxidation details; modeling
339 details; reaction mechanisms.

340 **Corresponding Author**

341 *Sarah S. Petters, spetters@unc.edu.

342 **Present Addresses**

343 †now at Institut de Recherches sur la Catalyse et l'Environnement de Lyon (IRCELYON), CNRS, and
344 Université Lyon 1, Villeurbanne, 69626 France.

345 **Funding Sources**

346 This project was funded by the U.S. National Science Foundation Postdoctoral Fellowship under
347 Award #AGS-1624696. REHM was supported by the U.K. Engineering and Physical Sciences
348 Research Council, grant number EP/N025245/1. ST and BJT were supported by the U. S.
349 National Oceanic and Atmospheric Administration under Award #NA16OAR4310106. We
350 thank Sara Duncan for assistance with some of the experiments.

351 **5. References**

352 (1) Mao, J.; Carlton, A.; Cohen, R. C.; Brune, W. H.; Brown, S. S.; Wolfe, G. M.; Jimenez, J. L.; Pye, H. O. T.; Lee Ng, N.; Xu, L.; McNeill, V. F.; Tsagaridis, K.; McDonald, B. C.; Warneke, C.; Guenther, A.; Alvarado, M. J.; de Gouw, J.; Mickley, L. J.; Leibensperger, E. M.; Mathur, R.; Nolte, C. G.; Portmann, R. W.; Unger, N.; Tosca, M.; Horowitz, L. W. Southeast Atmosphere Studies: Learning from Model-Observation Syntheses. *Atmos. Chem. Phys.* **2018**, *18* (4), 2615–2651. doi: 10.5194/acp-18-2615-2018.

353 (2) Chan Miller, C.; Jacob, D. J.; Marais, E. A.; Yu, K.; Travis, K. R.; Kim, P. S.; Fisher, J. A.; Zhu, L.; Wolfe, G. M.; Hanisco, T. F.; Keutsch, F. N.; Kaiser, J.; Min, K.-E.; Brown, S. S.; Washenfelder, R. A.; González Abad, G.; Chance, K. Glyoxal Yield from Isoprene Oxidation and Relation to Formaldehyde: Chemical Mechanism, Constraints from SENEX Aircraft Observations, and Interpretation of OMI Satellite Data. *Atmos. Chem. Phys.* **2017**, *17* (14), 8725–8738. doi: 10.5194/acp-17-8725-2017.

1
2
3
4
5
6
7
8
9
10
11
12
13
14
15
16
17
18
19
20
21
22
23
24
25
26
27
28
29
30
31
32
33
34
35
36
37
38
39
40
41
42
43
44
45
46
47
48
49
50
51
52
53
54
55
56
57
58
59
60
Manuscript for submission to *ACS Earth and Space Chemistry*

364 (3) Marais, E. A.; Jacob, D. J.; Jimenez, J. L.; Campuzano-Jost, P.; Day, D. A.; Hu, W.;
365 Krechmer, J.; Zhu, L.; Kim, P. S.; Miller, C. C.; Fisher, J. A.; Travis, K.; Yu, K.; Hanisco,
366 T. F.; Wolfe, G. M.; Arkinson, H. L.; Pye, H. O. T.; Froyd, K. D.; Liao, J.; McNeill, V. F.
367 Aqueous-Phase Mechanism for Secondary Organic Aerosol Formation from Isoprene:
368 Application to the Southeast United States and Co-Benefit of SO₂ Emission Controls.
369 *Atmos. Chem. Phys.* **2016**, *16* (3), 1603–1618. doi: 10.5194/acp-16-1603-2016.

370 (4) Ervens, B.; Turpin, B. J.; Weber, R. J. Secondary Organic Aerosol Formation in Cloud
371 Droplets and Aqueous Particles (AqSOA): A Review of Laboratory, Field and Model
372 Studies. *Atmos. Chem. Phys.* **2011**, *11* (21), 11069–11102. doi: 10.5194/acp-11-11069-
373 2011.

374 (5) Blando, J. D.; Turpin, B. J. Secondary Organic Aerosol Formation in Cloud and Fog
375 Droplets: A Literature Evaluation of Plausibility. *Atmos. Environ.* **2000**, *34* (10), 1623–
376 1632. doi: 10.1016/S1352-2310(99)00392-1.

377 (6) Budisulistiorini, S. H.; Canagaratna, M. R.; Croteau, P. L.; Marth, W. J.; Baumann, K.;
378 Edgerton, E. S.; Shaw, S. L.; Knipping, E. M.; Worsnop, D. R.; Jayne, J. T.; Gold, A.;
379 Surratt, J. D. Real-Time Continuous Characterization of Secondary Organic Aerosol
380 Derived from Isoprene Epoxydiols in Downtown Atlanta, Georgia, Using the Aerodyne
381 Aerosol Chemical Speciation Monitor. *Environ. Sci. Technol.* **2013**, *47* (11), 5686–5694.
382 doi: 10.1021/es400023n.

383 (7) McVay, R.; Ervens, B. A Microphysical Parameterization of AqSOA and Sulfate Formation
384 in Clouds. *Geophys. Res. Lett.* **2017**, *44* (14), 7500–7509. doi: 10.1002/2017GL074233.

385 (8) Woo, J. L.; McNeill, V. F. SimpleGAMMA v1.0 – a Reduced Model of Secondary Organic
386 Aerosol Formation in the Aqueous Aerosol Phase (AaSOA). *Geosci. Model Dev.* **2015**, *8*
387 (6), 1821–1829. doi: 10.5194/gmd-8-1821-2015.

388 (9) Heald, C. L.; Coe, H.; Jimenez, J. L.; Weber, R. J.; Bahreini, R.; Middlebrook, A. M.;
389 Russell, L. M.; Jolley, M.; Fu, T.-M.; Allan, J. D.; Bower, K. N.; Capes, G.; Crosier, J.;
390 Morgan, W. T.; Robinson, N. H.; Williams, P. I.; Cubison, M. J.; DeCarlo, P. F.; Dunlea, E.
391 J. Exploring the Vertical Profile of Atmospheric Organic Aerosol: Comparing 17 Aircraft
392 Field Campaigns with a Global Model. *Atmos. Chem. Phys.* **2011**, *11* (24), 12673–12696.
393 doi: 10.5194/acp-11-12673-2011.

394 (10) Carlton, A. G.; Turpin, B. J.; Altieri, K. E.; Seitzinger, S. P.; Mathur, R.; Roselle, S. J.;
395 Weber, R. J. CMAQ Model Performance Enhanced When In-Cloud Secondary Organic
396 Aerosol Is Included: Comparisons of Organic Carbon Predictions with Measurements.
397 *Environ. Sci. Technol.* **2008**, *42* (23), 8798–8802. doi: 10.1021/es801192n.

398 (11) Fu, T.-M.; Jacob, D. J.; Wittrock, F.; Burrows, J. P.; Vrekoussis, M.; Henze, D. K. Global
399 Budgets of Atmospheric Glyoxal and Methylglyoxal, and Implications for Formation of
400 Secondary Organic Aerosols. *J. Geophys. Res.: Atmos.* **2008**, *113* (D15303). doi:
401 10.1029/2007JD009505.

402 (12) Ortiz-Montalvo, D.; Häkkinen, S. A. K.; Schwier, A. N.; Lim, Y. B.; McNeill, V. F.; Turpin,
403 B. J. Ammonium Addition (and Aerosol PH) Has a Dramatic Impact on the Volatility and

1
2
3
4
5
6
7
8
9
10
11
12
13
14
15
16
17
18
19
20
21
22
23
24
25
26
27
28
29
30
31
32
33
34
35
36
37
38
39
40
41
42
43
44
45
46
47
48
49
50
51
52
53
54
55
56
57
58
59
60
Manuscript for submission to *ACS Earth and Space Chemistry*

404 Yield of Glyoxal Secondary Organic Aerosol. *Environ. Sci. Technol.* **2014**, *48* (1), 255–262.
405 doi: 10.1021/es4035667.

406 (13) Carlton, A. G.; Turpin, B. J.; Altieri, K. E.; Seitzinger, S.; Reff, A.; Lim, H.-J.; Ervens, B.
407 Atmospheric Oxalic Acid and SOA Production from Glyoxal: Results of Aqueous
408 Photooxidation Experiments. *Atmos. Environ.* **2007**, *41* (35), 7588–7602. doi:
409 10.1016/j.atmosenv.2007.05.035.

410 (14) Tan, Y.; Perri, M. J.; Seitzinger, S. P.; Turpin, B. J. Effects of Precursor Concentration and
411 Acidic Sulfate in Aqueous Glyoxal–OH Radical Oxidation and Implications for Secondary
412 Organic Aerosol. *Environ. Sci. Technol.* **2009**, *43* (21), 8105–8112. doi: 10.1021/es901742f.

413 (15) Perri, M. J.; Seitzinger, S.; Turpin, B. J. Secondary Organic Aerosol Production from
414 Aqueous Photooxidation of Glycolaldehyde: Laboratory Experiments. *Atmos. Environ.*
415 **2009**, *43* (8), 1487–1497. doi: 10.1016/j.atmosenv.2008.11.037.

416 (16) Ortiz-Montalvo, D.; Lim, Y. B.; Perri, M. J.; Seitzinger, S. P.; Turpin, B. J. Volatility and
417 Yield of Glycolaldehyde SOA Formed through Aqueous Photochemistry and Droplet
418 Evaporation. *Aerosol Sci. Technol.* **2012**, *46* (9), 1002–1014. doi:
419 10.1080/02786826.2012.686676.

420 (17) Michaud, V.; El Haddad, I.; Yao Liu; Sellegrí, K.; Laj, P.; Villani, P.; Picard, D.; Marchand,
421 N.; Monod, A. In-Cloud Processes of Methacrolein under Simulated Conditions – Part 3:
422 Hygroscopic and Volatility Properties of the Formed Secondary Organic Aerosol. *Atmos.*
423 *Chem. Phys.* **2009**, *9* (14), 5119–5130. doi: 10.5194/acp-9-5119-2009.

424 (18) Tan, Y.; Lim, Y. B.; Altieri, K. E.; Seitzinger, S. P.; Turpin, B. J. Mechanisms Leading to
425 Oligomers and SOA through Aqueous Photooxidation: Insights from OH Radical Oxidation
426 of Acetic Acid and Methylglyoxal. *Atmos. Chem. Phys.* **2012**, *12* (2), 801–813. doi:
427 10.5194/acp-12-801-2012.

428 (19) Tan, Y.; Carlton, A. G.; Seitzinger, S. P.; Turpin, B. J. SOA from Methylglyoxal in Clouds
429 and Wet Aerosols: Measurement and Prediction of Key Products. *Atmos. Environ.* **2010**, *44*
430 (39), 5218–5226. doi: 10.1016/j.atmosenv.2010.08.045.

431 (20) Lim, Y. B.; Turpin, B. J. Laboratory Evidence of Organic Peroxide and Peroxyhemiacetal
432 Formation in the Aqueous Phase and Implications for Aqueous OH. *Atmos. Chem. Phys.*
433 **2015**, *15* (22), 12867–12877. doi: 10.5194/acp-15-12867-2015.

434 (21) Ortiz-Montalvo, D.; Schwier, A. N.; Lim, Y. B.; McNeill, V. F.; Turpin, B. J. Volatility of
435 Methylglyoxal Cloud SOA Formed through OH Radical Oxidation and Droplet
436 Evaporation. *Atmos. Environ.* **2016**, *130*, 145–152. doi: 10.1016/j.atmosenv.2015.12.013.

437 (22) Renard, P.; Reed Harris, A. E.; Rapf, R. J.; Ravier, S.; Demelas, C.; Coulomb, B.; Quivet,
438 E.; Vaida, V.; Monod, A. Aqueous Phase Oligomerization of Methyl Vinyl Ketone by
439 Atmospheric Radical Reactions. *J. Phys. Chem. C* **2014**, *118* (50), 29421–29430. doi:
440 10.1021/jp5065598.

441 (23) Yu, L.; Smith, J.; Laskin, A.; George, K. M.; Anastasio, C.; Laskin, J.; Dillner, A. M.;
442 Zhang, Q. Molecular Transformations of Phenolic SOA during Photochemical Aging in the
443 Aqueous Phase: Competition among Oligomerization, Functionalization, and

1
2
3
4
5
6
7
8
9
10
11
12
13
14
15
16
17
18
19
20
21
22
23
24
25
26
27
28
29
30
31
32
33
34
35
36
37
38
39
40
41
42
43
44
45
46
47
48
49
50
51
52
53
54
55
56
57
58
59
60
Manuscript for submission to *ACS Earth and Space Chemistry*

444 Fragmentation. *Atmos. Chem. Phys.* **2016**, *16* (7), 4511–4527. doi: 10.5194/acp-16-4511-2016.

445

446 (24) Altieri, K. E.; Carlton, A. G.; Lim, H.-J.; Turpin, B. J.; Seitzinger, S. P. Evidence for Oligomer Formation in Clouds: Reactions of Isoprene Oxidation Products. *Environ. Sci. Technol.* **2006**, *40* (16), 4956–4960. doi: 10.1021/es052170n.

447

448

449 (25) Carlton, A. G.; Turpin, B. J.; Lim, H.-J.; Altieri, K. E.; Seitzinger, S. Link between Isoprene and Secondary Organic Aerosol (SOA): Pyruvic Acid Oxidation Yields Low Volatility Organic Acids in Clouds. *Geophys. Res. Lett.* **2006**, *33* (6). doi: 10.1029/2005GL025374.

450

451

452 (26) Griffith, E. C.; Carpenter, B. K.; Shoemaker, R. K.; Vaida, V. Photochemistry of Aqueous Pyruvic Acid. *Proc. Natl. Acad. Sci. USA* **2013**, *110* (29), 11714. doi: 10.1073/pnas.1303206110.

453

454

455 (27) Bernard, F.; Ciuraru, R.; Boréave, A.; George, C. Photosensitized Formation of Secondary Organic Aerosols above the Air/Water Interface. *Environ. Sci. Technol.* **2016**, *50* (16), 8678–8686. doi: 10.1021/acs.est.6b03520.

456

457

458 (28) Rapf, R. J.; Perkins, R. J.; Dooley, M. R.; Kroll, J. A.; Carpenter, B. K.; Vaida, V. Environmental Processing of Lipids Driven by Aqueous Photochemistry of α -Keto Acids. *ACS Cent. Sci.* **2018**, *4* (5), 624–630. doi: 10.1021/acscentsci.8b00124.

459

460

461 (29) Galloway, M. M.; Powelson, M. H.; Sedehi, N.; Wood, S. E.; Millage, K. D.; Kononenko, J. A.; Rynaski, A. D.; De Haan, D. O. Secondary Organic Aerosol Formation during Evaporation of Droplets Containing Atmospheric Aldehydes, Amines, and Ammonium Sulfate. *Environ. Sci. Technol.* **2014**, *48* (24), 14417–14425. doi: 10.1021/es5044479.

462

463

464

465 (30) De Haan, D. O.; Corrigan, A. L.; Tolbert, M. A.; Jimenez, J. L.; Wood, S. E.; Turley, J. J. Secondary Organic Aerosol Formation by Self-Reactions of Methylglyoxal and Glyoxal in Evaporating Droplets. *Environ. Sci. Technol.* **2009**, *43* (21), 8184–8190. doi: 10.1021/es902152t.

466

467

468

469 (31) Surratt, J. D.; Chan, A. W. H.; Eddingsaas, N. C.; Chan, M.; Loza, C. L.; Kwan, A. J.; Hersey, S. P.; Flagan, R. C.; Wennberg, P. O.; Seinfeld, J. H. Reactive Intermediates Revealed in Secondary Organic Aerosol Formation from Isoprene. *Proc. Natl. Acad. Sci.* **2010**, *107* (15), 6640–6645. doi: 10.1073/pnas.0911114107.

470

471

472

473 (32) Lee, A. K. Y.; Zhao, R.; Li, R.; Liggio, J.; Li, S.-M.; Abbatt, J. P. D. Formation of Light Absorbing Organo-Nitrogen Species from Evaporation of Droplets Containing Glyoxal and Ammonium Sulfate. *Environ. Sci. Technol.* **2013**, *47* (22), 12819–12826. doi: 10.1021/es402687w.

474

475

476

477 (33) Ervens, B. Progress and Problems in Modeling Chemical Processing in Cloud Droplets and Wet Aerosol Particles. In *Multiphase Environmental Chemistry in the Atmosphere*; ACS Symposium Series; American Chemical Society, 2018; Vol. 1299, pp 327–345. doi: 10.1021/bk-2018-1299.ch016.

478

479

480

481 (34) Donahue, N. M.; Kroll, J. H.; Pandis, S. N.; Robinson, A. L. A Two-Dimensional Volatility Basis Set – Part 2: Diagnostics of Organic-Aerosol Evolution. *Atmos. Chem. Phys.* **2012**, *12* (2), 615–634. doi: 10.5194/acp-12-615-2012.

482

483

1
2
3
4
5
6
7
8
9
10
11
12
13
14
15
16
17
18
19
20
21
22
23
24
25
26
27
28
29
30
31
32
33
34
35
36
37
38
39
40
41
42
43
44
45
46
47
48
49
50
51
52
53
54
55
56
57
58
59
60
Manuscript for submission to *ACS Earth and Space Chemistry*

484 (35) Loeffler, K. W.; Koehler, C. A.; Paul, N. M.; De Haan, D. O. Oligomer Formation in
485 Evaporating Aqueous Glyoxal and Methyl Glyoxal Solutions. *Environ. Sci. Technol.* **2006**,
486 40 (20), 6318–6323. doi: 10.1021/es060810w.

487 (36) Barsanti, K. C.; Kroll, J. H.; Thornton, J. A. Formation of Low-Volatility Organic
488 Compounds in the Atmosphere: Recent Advancements and Insights. *J. Phys. Chem. Lett.*
489 **2017**, 8 (7), 1503–1511. doi: 10.1021/acs.jpclett.6b02969.

490 (37) Girod, M.; Moyano, E.; Campbell, D. I.; Cooks, R. G. Accelerated Bimolecular Reactions
491 in Microdroplets Studied by Desorption Electrospray Ionization Mass Spectrometry. *Chem.*
492 *Sci.* **2011**, 2 (3), 501–510. doi: 10.1039/C0SC00416B.

493 (38) Marsh, B. M.; Iyer, K.; Cooks, R. G. Reaction Acceleration in Electrospray Droplets: Size,
494 Distance, and Surfactant Effects. *J. Am. Soc. Mass Spectrom.* **2019**. doi: 10.1007/s13361-
495 019-02264-w.

496 (39) Bain, R. M.; Pulliam, C. J.; Thery, F.; Cooks, R. G. Accelerated Chemical Reactions and
497 Organic Synthesis in Leidenfrost Droplets. *Angew. Chem. Int. Ed.* **2016**, 55 (35), 10478–
498 10482. doi: 10.1002/anie.201605899.

499 (40) Badu-Tawiah, A. K.; Campbell, D. I.; Cooks, R. G. Reactions of Microsolvated Organic
500 Compounds at Ambient Surfaces: Droplet Velocity, Charge State, and Solvent Effects. *J.*
501 *Am. Soc. Mass Spectrom.* **2012**, 23 (6), 1077–1084. doi: 10.1007/s13361-012-0365-3.

502 (41) Nguyen, T. B.; Lee, P. B.; Updyke, K. M.; Bones, D. L.; Laskin, J.; Laskin, A.; Nizkorodov,
503 S. A. Formation of Nitrogen- and Sulfur-Containing Light-Absorbing Compounds
504 Accelerated by Evaporation of Water from Secondary Organic Aerosols. *J. Geophys. Res.:*
505 *Atmos.* **2012**, 117 (D1). doi: 10.1029/2011JD016944.

506 (42) Li, Y.; Yan, X.; Cooks, R. G. The Role of the Interface in Thin Film and Droplet Accelerated
507 Reactions Studied by Competitive Substituent Effects. *Angew. Chem. Int. Ed.* **2016**, 55 (10),
508 3433–3437. doi: 10.1002/anie.201511352.

509 (43) Zhong, J.; Kumar, M.; Francisco, J. S.; Zeng, X. C. Insight into Chemistry on Cloud/Aerosol
510 Water Surfaces. *Acc. Chem. Res.* **2018**, 51 (5), 1229–1237. doi:
511 10.1021/acs.accounts.8b00051.

512 (44) Eugene, A. J.; Pillar, E. A.; Colussi, A. J.; Guzman, M. I. Enhanced Acidity of Acetic and
513 Pyruvic Acids on the Surface of Water. *Langmuir* **2018**, 34 (31), 9307–9313. doi:
514 10.1021/acs.langmuir.8b01606.

515 (45) Narayan, S.; Muldoon, J.; Finn, M. G.; Fokin, V. V.; Kolb, H. C.; Sharpless, K. B. “On
516 Water”: Unique Reactivity of Organic Compounds in Aqueous Suspension. *Angew. Chem.*
517 *Int. Ed.* **2005**, 44 (21), 3275–3279. doi: 10.1002/anie.200462883.

518 (46) Donaldson, D. J.; Vaida, V. The Influence of Organic Films at the Air–Aqueous Boundary
519 on Atmospheric Processes. *Chem. Rev.* **2006**, 106 (4), 1445–1461. doi: 10.1021/cr040367c.

520 (47) Nishino, N.; Hollingsworth, S. A.; Stern, A. C.; Roeselová, M.; Tobias, D. J.; Finlayson-
521 Pitts, B. J. Interactions of Gaseous HNO₃ and Water with Individual and Mixed Alkyl Self-
522 Assembled Monolayers at Room Temperature. *Phys. Chem. Chem. Phys.* **2014**, 16 (6),
523 2358–2367. doi: 10.1039/C3CP54118E.

1
2
3
4
5
6
7
8
9
10
11
12
13
14
15
16
17
18
19
20
21
22
23
24
25
26
27
28
29
30
31
32
33
34
35
36
37
38
39
40
41
42
43
44
45
46
47
48
49
50
51
52
53
54
55
56
57
58
59
60
Manuscript for submission to *ACS Earth and Space Chemistry*

524 (48) Wingen, L. M.; Moskun, A. C.; Johnson, S. N.; Thomas, J. L.; Roeselová, M.; Tobias, D.
525 J.; Kleinman, M. T.; Finlayson-Pitts, B. J. Enhanced Surface Photochemistry in Chloride–
526 Nitrate Ion Mixtures. *Phys. Chem. Chem. Phys.* **2008**, *10* (37), 5668–5677. doi:
527 10.1039/B806613B.

528 (49) Stefan, M. I.; Bolton, J. R. Reinvestigation of the Acetone Degradation Mechanism in Dilute
529 Aqueous Solution by the UV/H₂O₂ Process. *Environ. Sci. Technol.* **1999**, *33* (6), 870–873.
530 doi: 10.1021/es9808548.

531 (50) Kawamura, K.; Tachibana, E.; Okuzawa, K.; Aggarwal, S. G.; Kanaya, Y.; Wang, Z. F.
532 High Abundances of Water-Soluble Dicarboxylic Acids, Ketocarboxylic Acids and α -
533 Dicarbonyls in the Mountaintop Aerosols over the North China Plain during Wheat Burning
534 Season. *Atmos. Chem. Phys.* **2013**, *13* (16), 8285–8302. doi: 10.5194/acp-13-8285-2013.

535 (51) Talbot, R. W.; Andreae, M. O.; Berresheim, H.; Jacob, D. J.; Beecher, K. M. Sources and
536 Sinks of Formic, Acetic, and Pyruvic Acids over Central Amazonia: 2. Wet Season. *J.
537 Geophys. Res.: Atmos.* **1990**, *95* (Journal Article), 16799–16811. doi:
538 10.1029/JD095iD10p16799.

539 (52) Praplan, A. P.; Hegyi-Gaeggeler, K.; Barmet, P.; Pfaffenberger, L.; Dommen, J.;
540 Baltensperger, U. Online Measurements of Water-Soluble Organic Acids in the Gas and
541 Aerosol Phase from the Photooxidation of 1,3,5-Trimethylbenzene. *Atmos. Chem. Phys.*
542 **2014**, *14* (16), 8665–8677. doi: 10.5194/acp-14-8665-2014.

543 (53) Mattila, J. M.; Brophy, P.; Kirkland, J.; Hall, S.; Ullmann, K.; Fischer, E. V.; Brown, S.;
544 McDuffie, E.; Tevlin, A.; Farmer, D. K. Tropospheric Sources and Sinks of Gas-Phase
545 Acids in the Colorado Front Range. *Atmos. Chem. Phys.* **2018**, *18* (16), 12315–12327. doi:
546 10.5194/acp-18-12315-2018.

547 (54) Andino, J. M.; Smith, J. N.; Flagan, R. C.; Goddard, W. A.; Seinfeld, J. H. Mechanism of
548 Atmospheric Photooxidation of Aromatics: A Theoretical Study. *J. Phys. Chem.* **1996**, *100*
549 (26), 10967–10980. doi: 10.1021/jp9529351.

550 (55) Veres, P.; Roberts, J. M.; Burling, I. R.; Warneke, C.; de Gouw, J.; Yokelson, R. J.
551 Measurements of Gas-Phase Inorganic and Organic Acids from Biomass Fires by Negative-
552 Ion Proton-Transfer Chemical-Ionization Mass Spectrometry. *J. Geophys. Res.: Atmos.*
553 **2010**, *115* (D23). doi: 10.1029/2010JD014033.

554 (56) Reed Harris, A. E.; Pajunoja, A.; Cazaunau, M.; Gratien, A.; Pangui, E.; Monod, A.;
555 Griffith, E. C.; Virtanen, A.; Doussin, J.-F.; Vaida, V. Multiphase Photochemistry of
556 Pyruvic Acid under Atmospheric Conditions. *J. Phys. Chem. A* **2017**, *121* (18), 3327–3339.
557 doi: 10.1021/acs.jpca.7b01107.

558 (57) Andreae, M. O.; Talbot, R. W.; Li, S.-M. Atmospheric Measurements of Pyruvic and Formic
559 Acid. *J. Geophys. Res.: Atmos.* **1987**, *92*, 6635–6641. doi: 10.1029/JD092iD06p06635.

560 (58) Guzmán, M. I.; Colussi, A. J.; Hoffmann, M. R. Photoinduced Oligomerization of Aqueous
561 Pyruvic Acid. *J. Phys. Chem. A* **2006**, *110* (10), 3619–3626. doi: 10.1021/jp056097z.

1
2
3
4
5
6
7
8
9
10
11
12
13
14
15
16
17
18
19
20
21
22
23
24
25
26
27
28
29
30
31
32
33
34
35
36
37
38
39
40
41
42
43
44
45
46
47
48
49
50
51
52
53
54
55
56
57
58
59
60
Manuscript for submission to *ACS Earth and Space Chemistry*

562 (59) Schaefer, T.; Schindelka, J.; Hoffmann, D.; Herrmann, H. Laboratory Kinetic and
563 Mechanistic Studies on the OH-Initiated Oxidation of Acetone in Aqueous Solution. *J.
564 Phys. Chem. A* **2012**, *116* (24), 6317–6326. doi: 10.1021/jp2120753.

565 (60) Healy, R. M.; Wenger, J. C.; Metzger, A.; Duplissy, J.; Kalberer, M.; Dommen, J.
566 Gas/Particle Partitioning of Carbonyls in the Photooxidation of Isoprene and 1,3,5-
567 Trimethylbenzene. *Atmos. Chem. Phys.* **2008**, *8* (12), 3215–3230. doi: 10.5194/acp-8-3215-
568 2008.

569 (61) Berglund, R. N.; Liu, B. Y. H. Generation of Monodisperse Aerosol Standards. *Environ.
570 Sci. Technol.* **1973**, *7* (2), 147–153. doi: 10.1021/es60074a001.

571 (62) Werner, F.; Ditas, F.; Siebert, H.; Simmel, M.; Wehner, B.; Pilewskie, P.; Schmeissner, T.;
572 Shaw, R. A.; Hartmann, S.; Wex, H.; Roberts, G. C.; Wendisch, M. Twomey Effect
573 Observed from Collocated Microphysical and Remote Sensing Measurements over Shallow
574 Cumulus. *J. Geophys. Res.: Atmos.* **2014**, *119* (3), 1534–1545. doi: 10.1002/2013JD020131.

575 (63) Barr, E. B.; Carpenter, R. L.; Newton, G. J. Improved Liquid Feed System for the Berglund-
576 Liu Vibrating Orifice Monodisperse Aerosol Generator. *Environ. Sci. Technol.* **1984**, *18* (9),
577 721–723. doi: 10.1021/es00127a016.

578 (64) Devarakonda, V.; Ray, A. K.; Kaiser, T.; Schweiger, G. Vibrating Orifice Droplet Generator
579 for Studying Fast Processes Associated with Microdroplets. *Aerosol Sci. Technol.* **1998**, *28*
580 (6), 531–547. doi: 10.1080/02786829808965544.

581 (65) Mavrogiannis, N.; Ibo, M.; Fu, X.; Crivellari, F.; Gagnon, Z. Microfluidics Made Easy: A
582 Robust Low-Cost Constant Pressure Flow Controller for Engineers and Cell Biologists.
583 *Biomicrofluidics* **2016**, *10* (3), 034107. doi: 10.1063/1.4950753.

584 (66) Petters, M. D.; Kreidenweis, S. M.; Prenni, A. J.; Sullivan, R. C.; Carrico, C. M.; Koehler,
585 K. A.; Ziemann, P. J. Role of Molecular Size in Cloud Droplet Activation. *Geophys. Res.
586 Lett.* **2009**, *36* (22), L22801. doi: 10.1029/2009GL040131.

587 (67) Petters, S. S.; Pagonis, D.; Claflin, M. S.; Levin, E. J. T.; Petters, M. D.; Ziemann, P. J.;
588 Kreidenweis, S. M. Hygroscopicity of Organic Compounds as a Function of Carbon Chain
589 Length and Carboxyl, Hydroperoxy, and Carbonyl Functional Groups. *J. Phys. Chem. A*
590 **2017**, *121* (27), 5164–5174. doi: 10.1021/acs.jpca.7b04114.

591 (68) Davies, J. F.; Haddrell, A. E.; Reid, J. P. Time-Resolved Measurements of the Evaporation
592 of Volatile Components from Single Aerosol Droplets. *Aerosol Sci. Technol.* **2012**, *46* (6),
593 666–677. doi: 10.1080/02786826.2011.652750.

594 (69) Rovelli, G.; Miles, R. E. H.; Reid, J. P.; Clegg, S. L. Accurate Measurements of Aerosol
595 Hygroscopic Growth over a Wide Range in Relative Humidity. *J. Phys. Chem. A* **2016**, *120*
596 (25), 4376–4388. doi: 10.1021/acs.jpca.6b04194.

597 (70) Su, Y.-Y.; Marsh, A.; Haddrell, A. E.; Li, Z.-M.; Reid, J. P. Evaporation Kinetics of Polyol
598 Droplets: Determination of Evaporation Coefficients and Diffusion Constants. *J. Geophys.
599 Res.: Atmos.* **2017**, *122* (22), 12,317–12,334. doi: 10.1002/2017JD027111.

600 (71) Dawson, K. W.; Petters, M. D.; Meskhidze, N.; Petters, S. S.; Kreidenweis, S. M.
601 Hygroscopic Growth and Cloud Droplet Activation of Xanthan Gum as a Proxy for Marine

1
2
3
4
5
6
7
8
9
10
11
12
13
14
15
16
17
18
19
20
21
22
23
24
25
26
27
28
29
30
31
32
33
34
35
36
37
38
39
40
41
42
43
44
45
46
47
48
49
50
51
52
53
54
55
56
57
58
59
60
Manuscript for submission to *ACS Earth and Space Chemistry*

602 Hydrogels. *J. Geophys. Res.: Atmos.* **2016**, *121* (19), 11803–11818. doi:
603 10.1002/2016JD025143.

604 (72) Tomaz, S.; Cui, T.; Chen, Y.; Sexton, K. G.; Roberts, J. M.; Warneke, C.; Yokelson, R. J.;
605 Surratt, J. D.; Turpin, B. J. Photochemical Cloud Processing of Primary Wildfire Emissions
606 as a Potential Source of Secondary Organic Aerosol. *Environ. Sci. Technol.* **2018**, *52* (19),
607 11027–11037. doi: 10.1021/acs.est.8b03293.

608 (73) van Pinxteren, D.; Fomba, K. W.; Mertes, S.; Müller, K.; Spindler, G.; Schneider, J.; Lee,
609 T.; Collett, J. L.; Herrmann, H. Cloud Water Composition during HCCT-2010: Scavenging
610 Efficiencies, Solute Concentrations, and Droplet Size Dependence of Inorganic Ions and
611 Dissolved Organic Carbon. *Atmos. Chem. Phys.* **2016**, *16* (5), 3185–3205. doi: 10.5194/acp-
612 16-3185-2016.

613 (74) Deguillaume, L.; Charbouillot, T.; Joly, M.; Vaitilingom, M.; Parazols, M.; Marinoni, A.;
614 Amato, P.; Delort, A.-M.; Vinatier, V.; Flossmann, A.; Chaumerliac, N.; Pichon, J. M.;
615 Houdier, S.; Laj, P.; Sellegrí, K.; Colomb, A.; Brigante, M.; Mailhot, G. Classification of
616 Clouds Sampled at the Puy de Dôme (France) Based on 10 Yr of Monitoring of Their
617 Physicochemical Properties. *Atmos. Chem. Phys.* **2014**, *14* (3), 1485–1506. doi:
618 10.5194/acp-14-1485-2014.

619 (75) Lim, Y. B.; Tan, Y.; Turpin, B. J. Chemical Insights, Explicit Chemistry, and Yields of
620 Secondary Organic Aerosol from OH Radical Oxidation of Methylglyoxal and Glyoxal in
621 the Aqueous Phase. *Atmos. Chem. Phys.* **2013**, *13* (17), 8651–8667. doi: 10.5194/acp-13-
622 8651-2013.

623 (76) Herrmann, H.; Hoffmann, D.; Schaefer, T.; Bräuer, P.; Tilgner, A. Tropospheric Aqueous-
624 Phase Free-Radical Chemistry: Radical Sources, Spectra, Reaction Kinetics and Prediction
625 Tools. *Chem. Phys. Phys. Chem.* **2010**, *11* (18), 3796–3822. doi: 10.1002/cphc.201000533.

626 (77) Arakaki, T.; Anastasio, C.; Kuroki, Y.; Nakajima, H.; Okada, K.; Kotani, Y.; Handa, D.;
627 Azechi, S.; Kimura, T.; Tsuhako, A.; Miyagi, Y. A General Scavenging Rate Constant for
628 Reaction of Hydroxyl Radical with Organic Carbon in Atmospheric Waters. *Environ. Sci.
Technol.* **2013**, *47* (15), 8196–8203. doi: 10.1021/es401927b.

630 (78) Ahn, K.-H.; Liu, B. Y. H. Particle Activation and Droplet Growth Processes in
631 Condensation Nucleus Counter—I. Theoretical Background. *J. Aerosol Sci.* **1990**, *21* (2),
632 249–261. doi: 10.1016/0021-8502(90)90008-L.

633 (79) Bilde, M.; Svenningsson, B.; Mønster, J.; Rosenørn, T. Even–Odd Alternation of
634 Evaporation Rates and Vapor Pressures of C3–C9 Dicarboxylic Acid Aerosols. *Environ.
Sci. Technol.* **2003**, *37* (7), 1371–1378. doi: 10.1021/es0201810.

636 (80) Hinds, W. C. *Aerosol Technology: Properties, Behavior, and Measurement of Airborne
Particles*, 2nd ed.; John Wiley and Sons: New York, 1999.

638 (81) Davis, E. J.; Ray, A. K. Submicron Droplet Evaporation in the Continuum and Non-
639 Continuum Regimes. *J. Aerosol Sci.* **1978**, *9* (5), 411–422. doi: 10.1016/0021-
640 8502(78)90003-4.

1
2
3
4
5
6
7
8
9
10
11
12
13
14
15
16
17
18
19
20
21
22
23
24
25
26
27
28
29
30
31
32
33
34
35
36
37
38
39
40
41
42
43
44
45
46
47
48
49
50
51
52
53
54
55
56
57
58
59
60
Manuscript for submission to *ACS Earth and Space Chemistry*

641 (82) Hirschfelder, J. O.; Curtiss, C. F.; Bird, R. B. *Molecular Theory of Gases and Liquids*; Wiley, 1967.

643 (83) Lim, H.-J.; Carlton, A. G.; Turpin, B. J. Isoprene Forms Secondary Organic Aerosol Through Cloud Processing: Model Simulations. *Environ. Sci. Technol.* **2005**, *39* (12), 4441–4446. doi: 10.1021/es048039h.

646 (84) Suda, S. R.; Petters, M. D. Accurate Determination of Aerosol Activity Coefficients at Relative Humidities up to 99% Using the Hygroscopicity Tandem Differential Mobility Analyzer Technique. *Aerosol Sci. Technol.* **2013**, *47* (9), 991–1000. doi: 10.1080/02786826.2013.807906.

650 (85) Suda, S. R.; Petters, M. D.; Matsunaga, A.; Sullivan, R. C.; Ziemann, P. J.; Kreidenweis, S. M. Hygroscopicity Frequency Distributions of Secondary Organic Aerosols. *J. Geophys. Res.: Atmos.* **2012**, *117* (D04207). doi: 10.1029/2011JD016823.

653 (86) Pocker, Y.; Meany, J. E.; Nist, B. J.; Zadorojny, C. Reversible Hydration of Pyruvic Acid. I. Equilibrium Studies. *J. Phys. Chem.* **1969**, *73* (9), 2879–2882. doi: 10.1021/j100843a015.

655 (87) Ziemann, P. J.; Atkinson, R. Kinetics, Products, and Mechanisms of Secondary Organic Aerosol Formation. *Chem. Soc. Rev.* **2012**, *41* (19), 6582–6605. doi: 10.1039/C2CS35122F.

657 (88) Herrmann, H.; Schaefer, T.; Tilgner, A.; Styler, S. A.; Weller, C.; Teich, M.; Otto, T. Tropospheric Aqueous-Phase Chemistry: Kinetics, Mechanisms, and Its Coupling to a Changing Gas Phase. *Chem. Rev.* **2015**, *115* (10), 4259–4334. doi: 10.1021/cr500447k.

660 (89) Chan, A. W. H.; Chan, M. N.; Surratt, J. D.; Chhabra, P. S.; Loza, C. L.; Crounse, J. D.; Yee, L. D.; Flagan, R. C.; Wennberg, P. O.; Seinfeld, J. H. Role of Aldehyde Chemistry and NO_x Concentrations in Secondary Organic Aerosol Formation. *Atmos. Chem. Phys.* **2010**, *10* (15), 7169–7188. doi: 10.5194/acp-10-7169-2010.

664 (90) Jaoui, M.; Edney, E. O.; Kleindienst, T. E.; Lewandowski, M.; Offenberg, J. H.; Surratt, J. D.; Seinfeld, J. H. Formation of Secondary Organic Aerosol from Irradiated α -Pinene/Toluene/NO_x Mixtures and the Effect of Isoprene and Sulfur Dioxide. *J. Geophys. Res.: Atmos.* **2008**, *113* (D9). doi: 10.1029/2007JD009426.

668 (91) Liggio, J.; Li, S.-M.; McLaren, R. Heterogeneous Reactions of Glyoxal on Particulate Matter: Identification of Acetals and Sulfate Esters. *Environ. Sci. Technol.* **2005**, *39* (6), 1532–1541. doi: 10.1021/es048375y.

671 (92) Sanz, M. T.; Gmehling, J. Esterification of Acetic Acid with Isopropanol Coupled with Pervaporation: Part I: Kinetics and Pervaporation Studies. *Chem. Eng. J.* **2006**, *123* (1), 1–8. doi: 10.1016/j.cej.2006.06.006.

674 (93) Rathod, A. P.; Wasewar, K. L.; Sonawane, S. S. Enhancement of Esterification Reaction by Pervaporation Reactor: An Intensifying Approach. *Procedia Eng.* **2013**, *51*, 330–334. doi: 10.1016/j.proeng.2013.01.045.

677 (94) Barsanti, K. C.; Pankow, J. F. Thermodynamics of the Formation of Atmospheric Organic Particulate Matter by Accretion Reactions—Part 1: Aldehydes and Ketones. *Atmos. Environ.* **2004**, *38* (26), 4371–4382. doi: 10.1016/j.atmosenv.2004.03.035.

1
2
3
4
5
6
7
8
9
10
11
12
13
14
15
16
17
18
19
20
21
22
23
24
25
26
27
28
29
30
31
32
33
34
35
36
37
38
39
40
41
42
43
44
45
46
47
48
49
50
51
52
53
54
55
56
57
58
59
60
Manuscript for submission to *ACS Earth and Space Chemistry*

680 (95) Tong, C.; Blanco, M.; Goddard, W. A.; Seinfeld, J. H. Secondary Organic Aerosol
681 Formation by Heterogeneous Reactions of Aldehydes and Ketones: A Quantum Mechanical
682 Study. *Environ. Sci. Technol.* **2006**, *40* (7), 2333–2338. doi: 10.1021/es0519785.

683 (96) Krizner, H. E.; De Haan, D. O.; Kua, J. Thermodynamics and Kinetics of Methylglyoxal
684 Dimer Formation: A Computational Study. *J. Phys. Chem. A* **2009**, *113* (25), 6994–7001.
685 doi: 10.1021/jp903213k.

686 (97) Rapf, R. J.; Dooley, M. R.; Kappes, K.; Perkins, R. J.; Vaida, V. PH Dependence of the
687 Aqueous Photochemistry of α -Keto Acids. *J. Phys. Chem. A* **2017**, *121* (44), 8368–8379.
688 doi: 10.1021/acs.jpca.7b08192.

689 (98) Perkins, R. J.; Shoemaker, R. K.; Carpenter, B. K.; Vaida, V. Chemical Equilibria and
690 Kinetics in Aqueous Solutions of Zymonic Acid. *J. Phys. Chem. A* **2016**, *120* (51), 10096–
691 10107. doi: 10.1021/acs.jpca.6b10526.

692 (99) Otto, T.; Stieger, B.; Mettke, P.; Herrmann, H. Tropospheric Aqueous-Phase Oxidation of
693 Isoprene-Derived Dihydroxycarbonyl Compounds. *J. Phys. Chem. A* **2017**, *121* (34), 6460–
694 6470. doi: 10.1021/acs.jpca.7b05879.

695 (100) Mellouki, A.; Mu, Y. On the Atmospheric Degradation of Pyruvic Acid in the Gas Phase.
696 *Atmospheric Photochem.* **2003**, *157* (2), 295–300. doi: 10.1016/S1010-6030(03)00070-4.

697 (101) Sander, R. Compilation of Henry's Law Constants (Version 4.0) for Water as Solvent.
698 *Atmos. Chem. Phys.* **2015**, *15* (8), 4399–4981. doi: 10.5194/acp-15-4399-2015.

699 (102) Epstein, S. A.; Nizkorodov, S. A. A Comparison of the Chemical Sinks of Atmospheric
700 Organics in the Gas and Aqueous Phase. *Atmos. Chem. Phys.* **2012**, *12* (17), 8205–8222.
701 doi: 10.5194/acp-12-8205-2012.

702 (103) Stull, D. R. Inorganic Compounds. *Ind. Eng. Chem.* **1947**, *39* (4), 540–550. doi:
703 10.1021/ie50448a023.

704 (104) Emel'yanenko, V. N.; Turovtsev, V. V.; Fedina, Y. A. Thermodynamic Properties of
705 Pyruvic Acid and Its Methyl Ester. *Thermochim. Acta* **2018**, *665* (Journal Article), 70–75.
706 doi: 10.1016/j.tca.2018.05.009.

707 (105) Soonsin, V.; Zardini, A. A.; Marcolli, C.; Zuend, A.; Krieger, U. K. The Vapor Pressures
708 and Activities of Dicarboxylic Acids Reconsidered: The Impact of the Physical State of the
709 Aerosol. *Atmos. Chem. Phys.* **2010**, *10* (23), 11753–11767. doi: 10.5194/acp-10-11753-
710 2010.

711 (106) Booth, A. M.; Barley, M. H.; Topping, D. O.; McFiggans, G.; Garforth, A.; Percival, C. J.
712 Solid State and Sub-Cooled Liquid Vapour Pressures of Substituted Dicarboxylic Acids
713 Using Knudsen Effusion Mass Spectrometry (KEMS) and Differential Scanning
714 Calorimetry. *Atmos. Chem. Phys.* **2010**, *10* (10), 4879–4892. doi: 10.5194/acp-10-4879-
715 2010.

716 (107) Paciga, A. L.; Riipinen, I.; Pandis, S. N. Effect of Ammonia on the Volatility of Organic
717 Diacids. *Environ. Sci. Technol.* **2014**, *48* (23), 13769–13775. doi: 10.1021/es5037805.

1
2
3
4
5
6
7
8
9
10
11
12
13
14
15
16
17
18
19
20
21
22
23
24
25
26
27
28
29
30
31
32
33
34
35
36
37
38
39
40
41
42
43
44
45
46
47
48
49
50
51
52
53
54
55
56
57
58
59
60
Manuscript for submission to *ACS Earth and Space Chemistry*

718 (108) Pankow, J. F.; Asher, W. E. SIMPOL.1: A Simple Group Contribution Method for
719 Predicting Vapor Pressures and Enthalpies of Vaporization of Multifunctional Organic
720 Compounds. *Atmos. Chem. Phys.* **2008**, 8 (10), 2773–2796. doi: 10.5194/acp-8-2773-2008.

721 (109) Gordon, B. P.; Moore, F. G.; Scatena, L.; Richmond, G. L. On the Rise: Experimental and
722 Computational VSFS Studies of Pyruvic Acid and Its Surface Active Oligomer Species at
723 the Air-Water Interface. *J. Phys. Chem. A* **2019**. doi: 10.1021/acs.jpca.9b08854.

724 (110) Bilde, M.; Barsanti, K.; Booth, M.; Cappa, C. D.; Donahue, N. M.; Emanuelsson, E. U.;
725 McFiggans, G.; Krieger, U. K.; Marcolli, C.; Topping, D.; Ziemann, P.; Barley, M.; Clegg,
726 S.; Dennis-Smither, B.; Hallquist, M.; Hallquist, Å. M.; Khlystov, A.; Kulmala, M.;
727 Mogensen, D.; Percival, C. J.; Pope, F.; Reid, J. P.; Ribeiro, da S.; Rosenoern, T.; Salo, K.;
728 Soonsin, V. P.; Yli-Juuti, T.; Prisle, N. L.; Pagels, J.; Rarey, J.; Zardini, A. A.; Riipinen, I.
729 Saturation Vapor Pressures and Transition Enthalpies of Low-Volatility Organic Molecules
730 of Atmospheric Relevance: From Dicarboxylic Acids to Complex Mixtures. *Chem. Rev.*
731 **2015**, 115 (10), 4115–4156. doi: 10.1021/cr5005502.

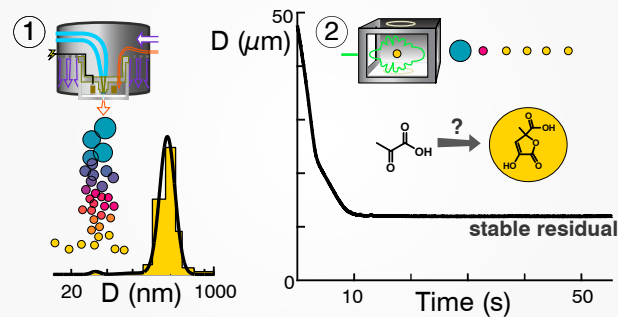
732

1
2
3
4
5
6
7
8
9
10
11
12
13
14
15
16
17
18
19
20
21
22
23
24
25
26
27
28
29
30
31
32
33
34
35
36
37
38
39
40
41
42
43
44
45
46
47
48
49
50
51
52
53
54
55
56
57
58
59
60
Manuscript for submission to *ACS Earth and Space Chemistry*733
734

735

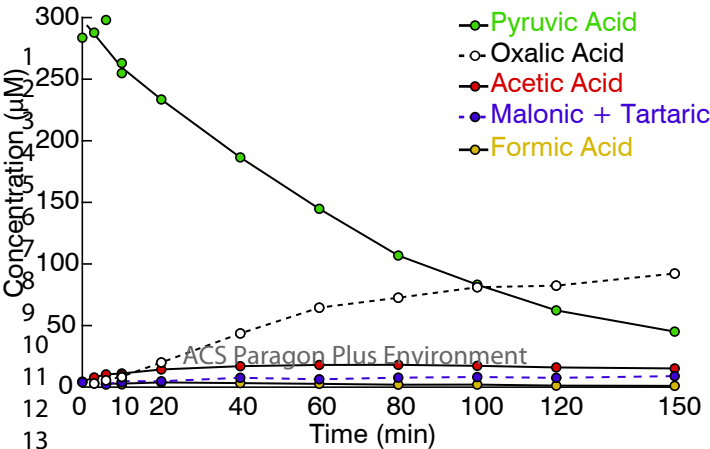
736

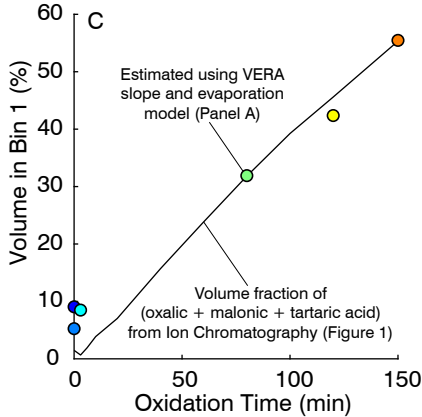
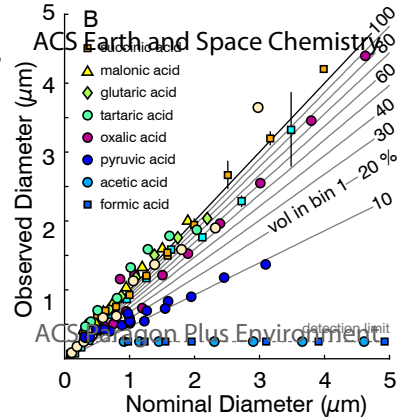
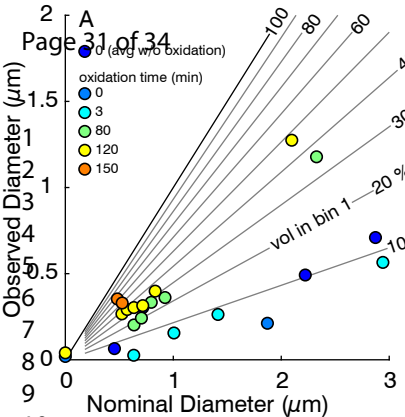
737

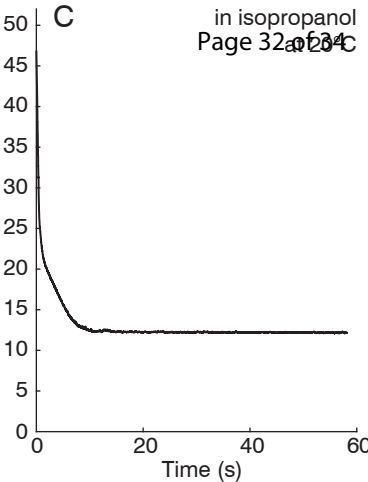
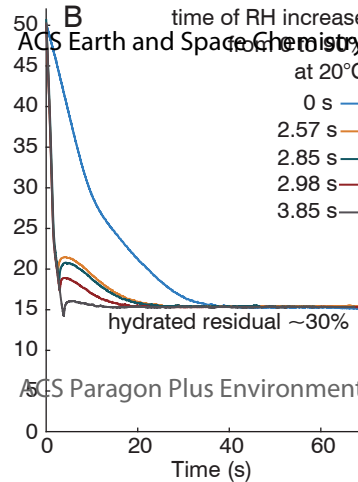
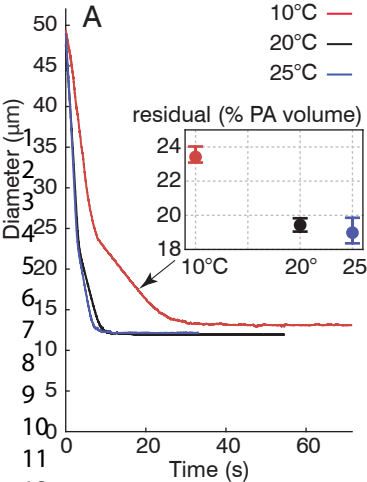
Pyruvic Acid in Evaporating Droplets

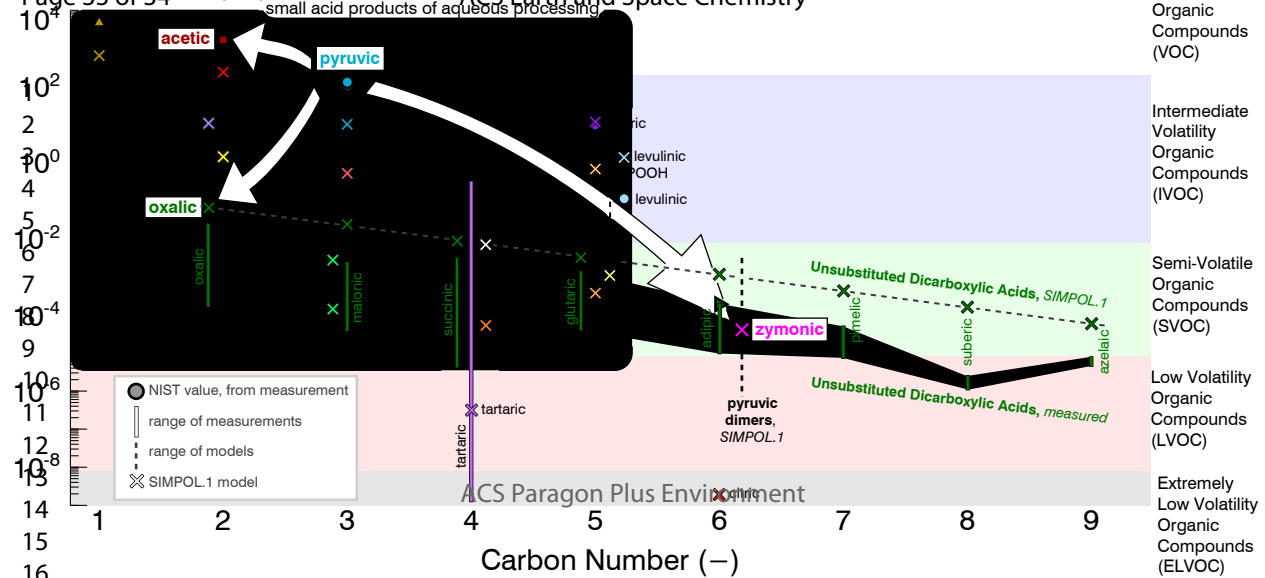
738

739
for TOC only









Intermediate Volatility Organic Compounds (IVOC)

Semi-Volatile Organic Compounds (SVOC)

Low Volatility Organic Compounds (LVOC)

Extremely Low Volatility Organic Compounds (ELVOC)

Pyruvic Acid in Evaporating Droplets

ACS Earth and Space Chemistry Page 34 of 34

